

Rotationally Resolved Electronic Spectra of *trans,trans*-Octatetraene and Its Derivatives

J. F. Pfanstiel and D. W. Pratt*

Department of Chemistry, University of Pittsburgh, Pittsburgh, Pennsylvania 15260

B. A. Tounge† and R. L. Christensen

Department of Chemistry, Bowdoin College, Brunswick, Maine 04011

Received: September 23, 1998; In Final Form: December 18, 1998

Described herein are the rotationally resolved one-photon fluorescence excitation spectra of several vibronic bands in the $S_1 \leftarrow S_0$ electronic transitions of three linear polyenes in the gas phase, 1,3,5,7-octatetraene (OT), 1,3,5,7-nonatetraene (NT), and 2,4,6,8-decatetraene (DT). Several of the spectra are significantly perturbed by an apparent centrifugal distortion in the S_1 state of OT, owing to the high frequency of rotations parallel to a and the low frequency of an in-plane bending mode (ν_{48}), by Coriolis coupling in the S_1 state of NT, involving ν_{48} and a nearby methyl torsional level, and by torsion–rotation coupling in the S_1 states of NT and DT, owing to a significant reduction in the excited-state torsional barrier(s) compared to the ground state. Nonetheless, the inertial parameters of eight different S_0 and S_1 vibronic levels have been determined, from which it is concluded that the carriers of the spectra are in all cases the *trans,trans* isomers. The important role of ν_{48} as a promoting mode for S_1 – S_2 vibronic coupling, the source of the $S_1 \leftarrow S_0$ oscillator strength, is confirmed. Finally, the measured differences in the rotational constants of the S_0 and S_1 states (e.g., $\Delta A = 2532$, $\Delta B = -11.7$, and $\Delta C = -11.0$ MHz for the vibronic origin of OT) provide new information about the changes in geometry that occur when the photon is absorbed.

Introduction

Polyenes (C_nH_{n+2}), molecules with alternating single and double bonds between covalently attached carbon atoms, are an important class of molecules with many interesting properties.¹ Among these is geometrical isomerism, by far the most significant property of polyenes in biological systems. Each 180° turn at either a single or a double bond gives a different configuration, resulting in a large number of possible structures, especially when n is large. Thus, octatetraene ($n = 8$) has 20 distinguishable isomers, although three or four consecutive *cis* configurations result in steric crowding that may prevent their formation. The net count in C_8H_{10} is 15, excluding *cis*³ configurations, and 18, excluding *cis*⁴ configurations.²

Given this fact, the existence of a controversy concerning the correct assignment of the electronic spectrum of octatetraene is not surprising. Heimbrook et al.³ observed $S_2 \rightarrow S_0$ ($1^1B_u \rightarrow 1^1A_g$) emission from the gas-phase molecule and recorded its strongly allowed $S_2 \leftarrow S_0$ fluorescence excitation spectrum. However, they were not able to detect the dipole forbidden $S_1 \leftrightarrow S_0$ ($2^1A_g \leftrightarrow 1^1A_g$) transition under isolated molecule conditions. Later, Buma et al.⁴ obtained the two-color REMPI spectrum of the 2^1A_g state in the gas phase and assigned their spectrum to a “*cis, trans*” isomer. They argued that only a noncentrosymmetric isomer would have a large enough oscillator strength to be detected under their experimental conditions. Then, Petek et al.⁵ succeeded in observing the $S_1 \rightarrow S_0$ fluorescence of octatetraene in a supersonic jet and recording

its one- and two-photon $S_1 \leftarrow S_0$ fluorescence excitation spectra. A detailed comparison of these spectra led to the conclusion that the carrier is the *trans,trans* isomer, the most stable form. This conclusion was supported by a more recent study of the fluorescence excitation spectra of two additional “linear” tetraenes, nontetraene and decatetraene, in which one or both terminal hydrogen atoms in octatetraene are replaced by methyl groups.^{6,7}

Rotationally resolved electronic spectroscopy is a powerful method for establishing the identity of gas-phase chromophores. The patterns of energy levels observed in this experiment are sensitive both to the size and shape of the molecule and to how these change when a photon is absorbed.⁸ Here, we demonstrate the utility of this approach in a study of the high-resolution one-photon fluorescence excitation spectra of octatetraene, nonatetraene, and decatetraene in the collision-free environment of a molecular beam. The results provide an unambiguous identification of the isomers responsible for the above-mentioned spectra as the *trans,trans* forms. The spectra also give new insight into the remarkable photochemical and photophysical properties of the polyenes and provide new experimental benchmarks for evaluating theoretical descriptions of their 2^1A_g states.

Experimental Section

Octatetraene (OT) was prepared by dehydrating 1,4,6-octatrien-3-ol at 80 °C using pyridinium *p*-toluenesulfonate (Aldrich) following the procedure developed by Yoshida and Tasumi.⁹ The 1,4-octatrien-3-ol was produced by mixing 2,4-hexadienal with vinylmagnesium bromide (Alfa). The dehydra-

* Corresponding author. Email: pratt+@pitt.edu.

† Present address: Department of Chemistry, Yale University, New Haven, CT 06511.

tion produces *trans,trans*-OT of >99% isomeric purity as determined by an analysis of the $S_2 \leftarrow S_0$ spectrum in a free jet.⁵ The OT crystals were stored at -80°C to preserve their isomeric purity. Nonatetraene (NT) and decatetraene (DT) were synthesized from Wittig reactions, using hexadienal and allyltriphenylphosphonium bromide (Fluka) for the former and hexadienal and crotyltriphenylphosphonium bromide (Fluka) for the latter.

Supersonic jet spectra were obtained using a standard low-resolution apparatus. Typically, the polyenes (OT at room temperature, NT and DT with mild heating) were seeded into 80 psig He and expanded through a pulsed 1 mm nozzle (General Valve, series 9). The resulting free jet was crossed with a frequency-doubled Quanta-Ray Nd^{3+} :YAG-pumped dye laser beam about 1 cm downstream of the nozzle. When tuned to a particular vibronic band in the absorption spectrum, the laser produced $S_1 \rightarrow S_0$ fluorescence, which was collected by a single lens system, detected by a photomultiplier tube and SRS boxcar integrator, and acquired by a MASSCOMP data acquisition system.

High-resolution spectra were obtained using a CW molecular beam spectrometer equipped with an intracavity-doubled Spectra-Physics ring dye laser, described in detail elsewhere.¹⁰ As above, OT at room temperature (or NT and DT with mild heating) was continuously expanded through a $90\ \mu\text{m}$ nozzle in 40–60 psig He, skimmed once, and excited ~ 15 cm downstream of the nozzle by the laser. Fluorescence was collected using spatially selective optics, detected by a photomultiplier tube and photon-counting system, and processed by the data acquisition system. Relative frequency calibrations of the spectra were performed using a near-confocal interferometer. Approximately 10×100 mg of each sample was available for the experiments, so special care was taken to optimize the performance of the apparatus prior to each run.

Results and Interpretation

Figure 1 shows the low-resolution one-photon fluorescence excitation spectra of OT, NT, and DT recorded in a supersonic jet. These are similar in every respect to the published spectra.^{4–7} The first strong band in the excitation spectrum of OT (Figure 1a) is at $29\ 024.9\ \text{cm}^{-1}$ (band OT-1). This band has been assigned as the 0_0^0 band of the $S_1 \leftarrow S_0$ transition of an OT having a *cis* linkage by Buma et al.⁴ and as the vibronic origin of *trans,trans*-OT by Petek et al.⁵ Their assignment places the 0_0^0 band at $76.2\ \text{cm}^{-1}$ to the red of band OT-1, at $28\ 948.7\ \text{cm}^{-1}$, observed only in two-photon excitation experiments.⁵ The frequency of $76.2\ \text{cm}^{-1}$ has been assigned to ν_{48} , a b_u in-plane bending mode in the S_1 state. Also prominent in the spectrum of OT is a band at $0_0^0 + 411.9\ \text{cm}^{-1}$ (band OT-2), which has been assigned to $\nu_{48} + \nu_{16}$, where ν_{16} is a totally symmetric (a_g) in-plane bending mode.

The first strong band in the excitation spectrum of NT (Figure 1b) is a doublet (bands NT-1 and NT-2). Band NT-1 lies at $28\ 950.8\ \text{cm}^{-1}$ and has been assigned as the true origin of the $S_1 \leftarrow S_0$ transition of *trans,trans*-NT.⁷ According to Petek et al.,⁷ the doubling of the origin is produced by the hindered internal rotation of the attached methyl group. Thus, the two components are $0a_1 \leftarrow 0a_1$ and $1e \leftarrow 1e$ tunneling doublets, with the latter (band NT-2) shifted to the blue by $3.34\ \text{cm}^{-1}$ with respect to the former (band NT-1). At $60.1\ \text{cm}^{-1}$ further to the blue of band NT-1 lies a second doublet (bands NT-3 and NT-4), also split (by $3.37\ \text{cm}^{-1}$) by the tunneling motion of the methyl group. Band NT-3 lies at $29\ 010.9\ \text{cm}^{-1}$ and has

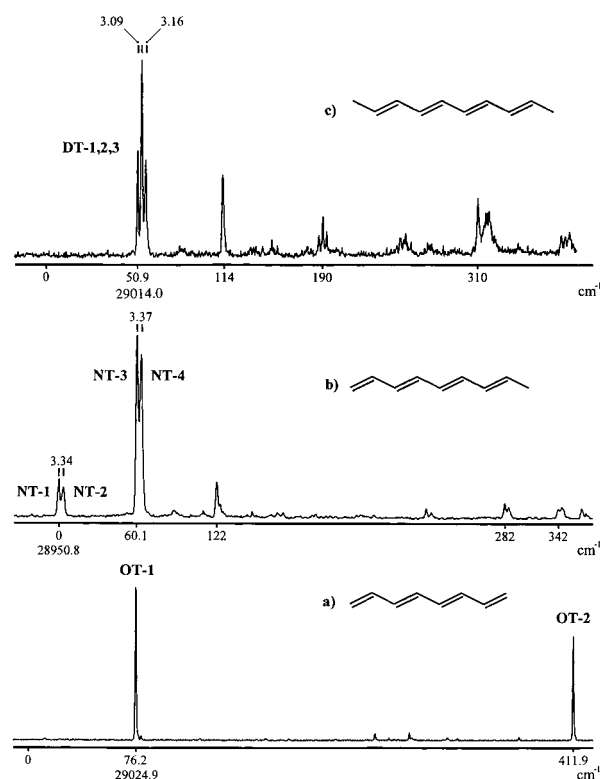


Figure 1. Low-resolution one-photon fluorescence excitation spectra of (a) octatetraene, (b) nonatetraene, and (c) decatetraene in a supersonic jet. The three spectra are aligned so that their vibronic origins coincide. Different horizontal energy scales are used in each spectrum.

been assigned as the vibronic origin of the $S_1 \leftarrow S_0$ transition of *trans,trans*-NT. Most (but not all) of the remaining bands in the low-resolution spectrum exhibit similar splittings.

The first strong band in the excitation spectrum of DT (Figure 1c) is a triplet (bands DT-1, 2, and 3). Band DT-1 is at $29\ 014.0\ \text{cm}^{-1}$. This band has been assigned as the vibronic origin of the $S_1 \leftarrow S_0$ transition of *trans,trans*-DT, whose true origin lies $50.9\ \text{cm}^{-1}$ to the red at $28\ 963.1\ \text{cm}^{-1}$.^{6,7} The three components of the triplet are separated by 3.09 and $3.16\ \text{cm}^{-1}$. These have been assigned as the $0a_1 \leftarrow 0a_1$, $1g \leftarrow 1g$, and $(1e_1 + 1e_3) \leftarrow (1e_1 + 1e_3)$ tunneling components of two equivalent methyl groups. Further to the blue in the spectra of all three molecules are several additional vibronic bands that have not been examined at high resolution. Their assignments are discussed elsewhere.^{4–7}

Figure 2 shows the rotationally resolved one-photon fluorescence excitation spectrum of the band at $29\ 024.9\ \text{cm}^{-1}$ in OT, band OT-1.¹¹ The spectrum is that of a near-prolate symmetric top ($\kappa = -0.999$) and, despite its overall appearance, is an a-type band. Band OT-2, at $29\ 360.6\ \text{cm}^{-1}$, is qualitatively similar. The reason for the unusual appearance of these two bands is that the *pseudolinear* OT has, in its S_0 state, a large A constant (~ 20 GHz) relative to its B and C constants (~ 500 MHz). The moment of inertia about the long axis is very small relative to those perpendicular to it. Thus, OT is very nearly a symmetric top. Even a very small percentage change in the A constant on electronic excitation produces large shifts in the individual K_a subbands, as shown in Figure 3. These shifts are approximately proportional to K_a^2 , destroying the sharp, centrally located Q-branch structure that is normally observed in a-type bands. Similar effects have been observed in the rotationally resolved $S_1 \leftarrow S_0$ spectra of *trans,trans*-diphenylbutadiene (DPB)¹² and *trans*-stilbene (*tS*).¹³

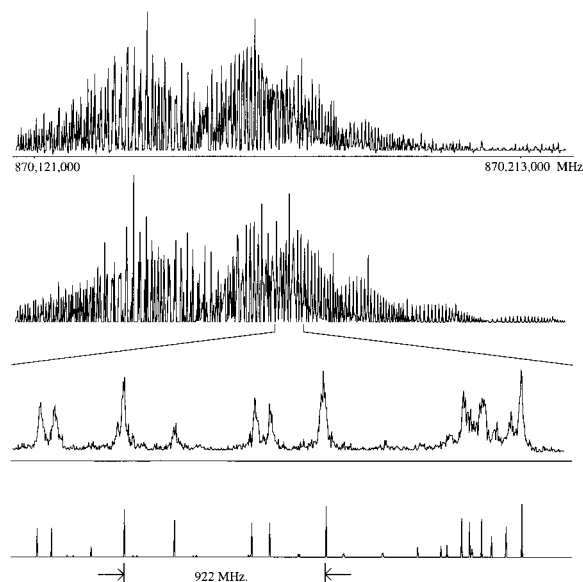


Figure 2. High-resolution one-photon fluorescence excitation spectrum of band OT-1 in the $S_1 \leftarrow S_0$ transition of octatetraene, at $29\,024.9\text{ cm}^{-1}$, in a molecular beam. The top trace shows the experimental spectrum, the next trace shows the computed spectrum (simulated using the constants in Tables 1 and 2), and the bottom two traces show a comparison of a portion of the experimental and computed spectra, to illustrate the quality of the fit. The line width of single rovibronic features in the experimental spectrum is 15 MHz; this line width is not included in the simulation in the bottom trace. The rotational temperature of the fit is 8 K.

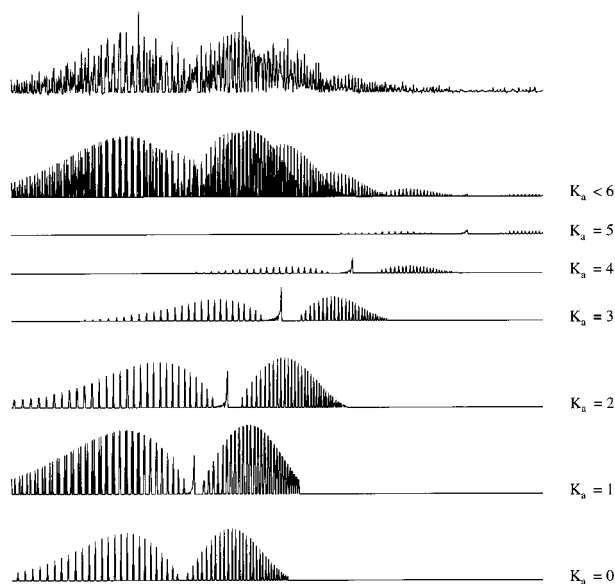


Figure 3. Deconvolution of the spectrum in Figure 2, showing the contributions from individual K_a subbands. Note the large shift to the blue of successive subbands, determined by $\Delta(A-B)K_a^2$ in the rigid-rotor limit. These shifts are increased further by the addition of the $D_K K_a^4$ distortion term to the S_1 Hamiltonian.

The parameters obtained from fits of these two spectra to distortable rotor Hamiltonians (S-reduction)¹⁴ are listed in Tables 1 and 2. Bands OT-1 and OT-2 exhibit the same ground-state rotational constants within experimental error. Thus, they both originate in the same vibronic level, presumably the zero-point vibrational level (ZPL) of the S_0 state. The ground-state parameters listed in Table 1 are the results of a fit of 205 combination differences obtained from the two spectra. The calculated energy differences reproduce the experimental values to within a standard deviation of 4.5 MHz. This may be

TABLE 1: Inertial Parameters of trans,trans-Octatetraene in the Zero-Point Vibrational Level of Its Ground Electronic State (1^1A_g)

	experiment		theory	
	expt ^a	std error ^b	HF(6-31G*)	CASSCF ^c
A'' (MHz)	18192	1242	19831	19738
B'' (MHz)	571.04(0.1)	0.05	573.2	568.0
C'' (MHz)	554.96(0.1)	0.04	557.1	552.2
κ''	-0.999		-0.999	-0.998
$\Delta I''$ (amu \AA^2)	-2.14	1.91	0.0	0.0

^a Results from a fit of 205 combination-differences that appear in the rotationally resolved spectra of the two bands at $29\,024.9\text{ cm}^{-1}$ ($0_0^0 + 76.2\text{ cm}^{-1}$) and $29\,360.6\text{ cm}^{-1}$ ($0_0^0 + 411.9\text{ cm}^{-1}$). Numbers in parentheses represent estimates of the systematic uncertainties in the experiment. ^b Estimated errors from the diagonal elements of the correlation matrix. ^c Reference 16.

TABLE 2: Inertial Parameters of trans,trans-Octatetraene in Two Vibrational Levels of Its First Excited Electronic State (2^1A_g)

	$0_0^0 + 76.2\text{ cm}^{-1}$		$0_0^0 + 411.9\text{ cm}^{-1}$		theoretical
	expt ^a	std error ^b	expt ^a	std error ^b	CASSCF ^c
A' (MHz)	20724	2000	20435	2000	19649
B' (MHz)	559.29(0.1)	0.01	559.30(0.1)	0.01	555.8
C' (MHz)	543.96(0.1)	0.01	543.93(0.1)	0.01	540.5
D_J' (Hz)	16.6	0.4	44	2	
D_{JK}' (Hz)	2310	51	583	289	
D_K' (MHz)	10.35	0.01	13.68	0.05	
d_1' (Hz)	3.9	0.1	25	2	
d_2' (Hz)	1.8	0.2	5	2	
κ'	-0.998		-0.998		-0.998
$\Delta I'$ (amu \AA^2) ^d	1.08	0.01	0.80	0.01	0.0
assign	353		192		
rms (OMC)	11.0		7.2		

^a Numbers in parentheses represent estimates of the systematic uncertainties in the experiment. Band origins were not determined owing to the lack of a calibrated I_2 spectrum in this region. ^b Estimated errors from the diagonal elements of the correlation matrix. ^c Reference 16. ^d Neglecting distortion parameters.

compared to the observed Doppler width of about 15 MHz. Adding centrifugal distortion terms to the S_0 Hamiltonian did not significantly improve the quality of the fit. Hence, the ZPL of the ground state is a rigid rotor.

Also listed in Table 1 are two sets of theoretical rotational constants for the trans,trans isomer of OT. The first set was calculated from a Hartree-Fock (HF) geometry, optimized using the 6-31G* basis set.¹⁵ It gives $A'' = 19\,831$, $B'' = 573$, and $C'' = 557$ MHz. The second set was calculated from a geometry obtained by Serrano-Andrés et al.¹⁶ using the complete active-space self-consistent-field (CASSCF) method. It gives very similar values: $A'' = 19\,738$, $B'' = 568$, and $C'' = 552$ MHz. The experimental A'' rotational constant (18 192 MHz) could not be determined accurately from the spectra owing to their near-symmetric-top nature.¹⁷ However, the experimental values of B'' (571 MHz) and C'' (555 MHz) are known to high precision. Moreover, there is near-perfect agreement between these values and the two sets of theoretical values. We therefore conclude that the carrier responsible for the two observed bands is trans,trans-OT, in agreement with Petek et al.⁵

We also have calculated the rotational constants of eight additional OT isomers, each possessing at least one cis linkage, using the 6-31G* basis set. All exhibit significantly smaller A'' values and significantly larger B'' and C'' values, as expected. For example, the tctt isomer has $A'' = 8019$, $B'' = 758$, and $C'' = 693$ MHz.¹⁸ Thus, there can be little doubt that the carrier of these bands is the trans,trans structure.

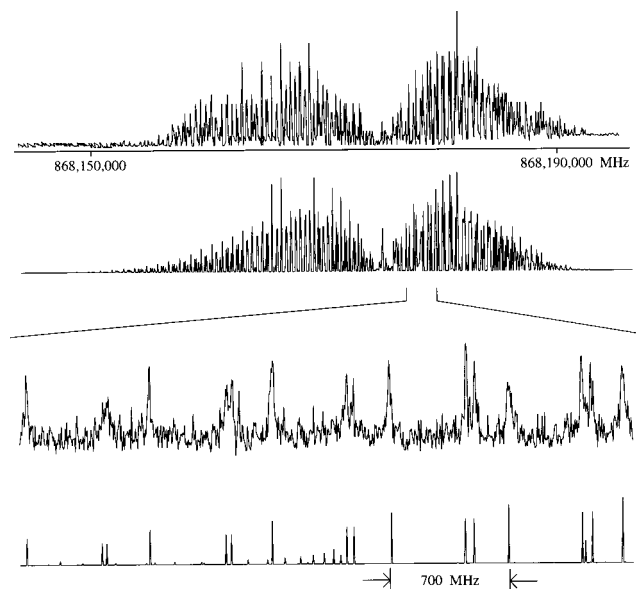


Figure 4. High-resolution one-photon fluorescence excitation spectrum of band NT-1 in the $S_1 \leftarrow S_0$ transition of nonatetraene, at $28\,950.8\text{ cm}^{-1}$, in a molecular beam. See the captions to Figures 2 and 3 for more details. The rotational temperature of the fit is 4 K.

The excited-state parameters of the two bands listed in Table 2 were determined separately by fixing the S_0 rotational constants at the experimental values shown in Table 1 and varying the S_1 rotational constants to obtain least-squares fits. These calculations showed that both excited-state vibrational levels are nonrigid, requiring the full Watson Hamiltonian¹⁴ for their analysis. For the band at $0_0^0 + 76.2\text{ cm}^{-1}$ (band OT-1), we fit 353 transitions with a standard deviation of 11.0 MHz. For the band at $0_0^0 + 411.9\text{ cm}^{-1}$ (band OT-2), we fit 192 transitions with a standard deviation of 7.2 MHz. Both deviations are less than the observed widths of single rovibronic lines in the two spectra. The complete set of quartic centrifugal distortion terms¹⁴ is listed in Table 2. However, only $D_{K'}$ significantly improves the fit. The effect of this term is to shift the parallel-type K_a subbands even further to the blue, by $D_{K'}K_a^4$ (cf., Figure 3). No other perturbations were observed in these two rotationally resolved spectra of OT.

Four bands in the $S_1 \leftarrow S_0$ spectrum of NT have been recorded at high resolution. These include both components of the doublet located at $28\,950.8$ and $28\,954.1\text{ cm}^{-1}$ (bands NT-1 and NT-2) and both components of the doublet located at $29\,010.9$ and $29\,014.3\text{ cm}^{-1}$ (bands NT-3 and NT-4). These are shown in Figures 4–6. The red and blue members of the doublets have been assigned to torsional levels having a and e symmetry, respectively.⁷ Consistent with this interpretation, bands NT-1 and NT-3 were found to exhibit a-type contours, like the two recorded bands of OT. Thus, similar strategies could be used for their analysis. First, we fit the two bands independently, using rigid rotor Hamiltonians for all four states. Again, we found near-prolate symmetric top behavior, with large A and small and nearly equal B and C values. We also found that the two sets of ground-state constants are identical within experimental error, showing that the two bands originate in the same vibronic level, presumably the ZPL of the S_0 state. Then we used the combination–difference method to determine more accurate values of the rotational constants of this level. The results are listed in Table 3. Examination of these data shows that, in its ground state, NT is very nearly a planar symmetric top ($\kappa = -0.999$) to which a single methyl group is attached ($\Delta I = -3.3\text{ amu \AA}^2$). The data also show that the S_0 ZPL of NT is rigid; adding centrifugal distortion terms did not significantly improve the quality of the fit.

As a substituted polyene, NT also can exhibit the property of geometrical isomerism, leading to several possible structures. So again, it is important to compare our results with theory to ascertain which isomer is responsible for the observed spectra. Two such comparisons are shown in Table 3, one using the rotational constants calculated by the HF (6-31G*) method and a second using the constants calculated by the CASSCF method, both sets referring to the *trans,trans* structure. (The second set of constants was determined by adding a methyl group to the optimized geometry of *trans,trans*-OT obtained by Serrano-Andrés et al.¹⁶) Again, we find excellent agreement between experiment and theory, showing that the carrier responsible for these two bands is *trans,trans*-NT.

The two S_1 vibrational levels reached in bands NT-1 and NT-3 have significantly different properties. As can be seen from Figure 4, the high-resolution spectrum of band NT-1

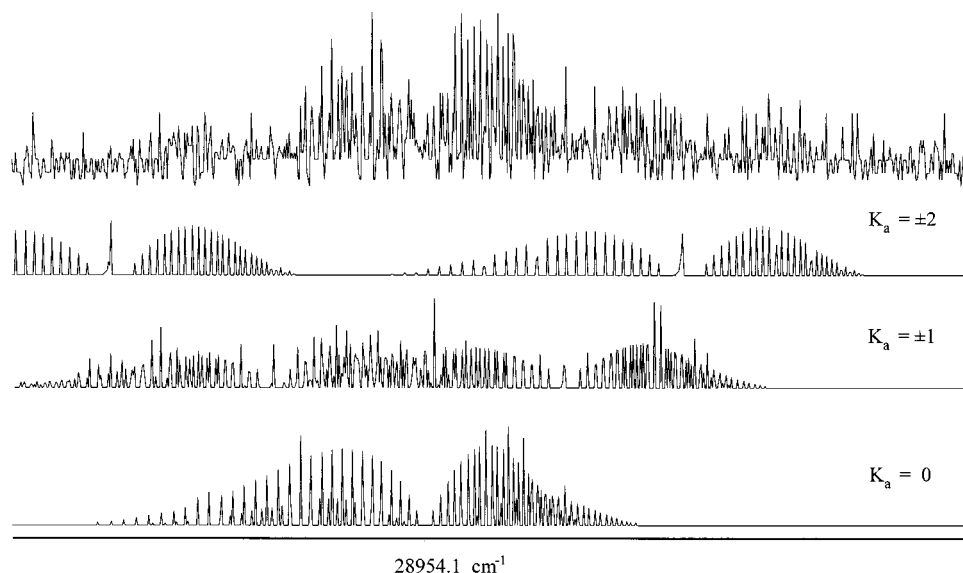


Figure 5. High-resolution one-photon fluorescence excitation spectrum of band NT-2 in the $S_1 \leftarrow S_0$ transition of nonatetraene, at $28\,954.1\text{ cm}^{-1}$, in a molecular beam and an approximate deconvolution of its K_a subband structure (cf. Figure 3). Note that the $K_a > 0$ transitions are split into two subbands. This splitting is approximately proportional to $D_a K_a$, where D_a is the coefficient of the linear angular momentum operator parallel to the a axis.

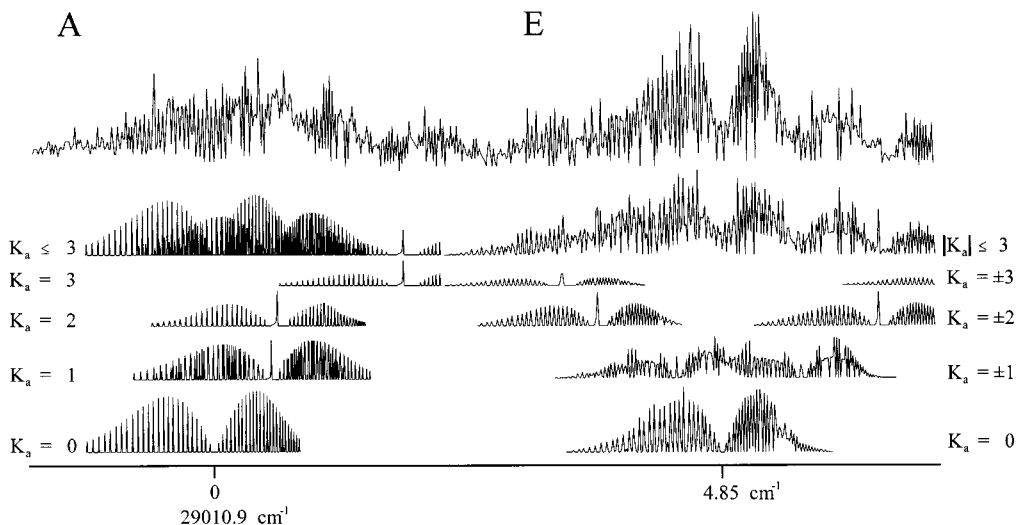


Figure 6. High-resolution one-photon fluorescence excitation spectra of bands NT-3 and NT-4 in the $S_1 \leftarrow S_0$ transition of nonatetraene in a molecular beam and an approximate deconvolution of their K_a subband structures (cf. Figures 3 and 5). The origin of band NT-3 is at $29\,010.9\text{ cm}^{-1}$. Note that the shifts of the K_a subbands are not monotonic in nature. See text for proposed explanation.

TABLE 3: Inertial Parameters of trans,trans-Nonatetraene in the $0a_1$ Torsional Component of the Zero-Point Level of Its Ground Electronic State (1A_g)

	experiment		theory	
	expt ^a	std error ^b	HF(6-31G*)	CASSCF ^c
A'' (MHz)	16302	2500	16579	16090
B'' (MHz)	390.42(0.1)	0.04	391.5	390.0
C'' (MHz)	382.25(0.1)	0.04	383.3	381.9
κ''	-0.999		-0.999	-0.999
$\Delta I''$ (amu \AA^2)	-3.3	4.8	-3.08	-3.76

^a Results from a fit of 192 combination-differences that appear in the rotationally resolved spectra of the two red components of the doublets in the 0_0^0 and $0_0^0 + 60.1\text{ cm}^{-1}$ bands, located at $28\,950.8$ and $29\,010.9\text{ cm}^{-1}$, respectively. Numbers in parentheses represent estimates of the systematic uncertainties in the experiment. ^b Estimated errors from the diagonal elements of the correlation matrix. ^c Estimated by addition of a methyl group to the OT geometry obtained by Serrano-Andrés et al. (ref 16).

exhibits the same large, monotonic shifts of its K_a subbands that were observed in bands OT-1 and OT-2 of trans,trans-OT, signaling a large change in the A rotational constant on S_1 excitation. However, a fit of band NT-1 to the distortable rotor Hamiltonian (using the ground-state constants listed in Table 3) revealed no significant additional shifts due to the $D_{K'}K_a^4$ distortion term, similar to those observed in OT. The S_1 vibrational level reached in band NT-1 is rigid. Its inertial parameters are listed in Table 4. These parameters include the quartic distortion terms, but these are relatively small and give only a slight improvement to the fit. We conclude from this observation that this level is the ZPL of the S_1 state, as suggested by Petek et al.⁷

The situation is different in band NT-3. Figure 6 shows its rotationally resolved spectrum (as well as that of band NT-4, vide infra). Transitions observed in this spectrum have been successfully assigned, as demonstrated by their use in the combination-difference calculations. However, these assignments showed that the observed K_a structure in band NT-3 does not conform to expectations for either a rigid rotor or a distortable rotor. In particular, as shown in Figure 6, the shift of the K_a subbands is not monotonic, proportional to either K_a^2 or K_a^4 or some combination thereof. Instead, the shifts of particular subbands appear to be larger for odd values of K_a .

TABLE 4: Inertial Parameters of trans,trans-Nonatetraene in the $0a_1$ Torsional Component of the Zero-Point Level of Its First Excited Electronic State (2A_g)

	experiment		theory
	expt ^a	std error ^b	CASSCF ^c
A' (MHz)	16759	2500	15796
B' (MHz)	384.05(0.1)	0.01	381.9
C' (MHz)	375.82(0.1)	0.01	374.0
D_j' (Hz)	-21	3	
D_{JK}' (kHz)	4.4	0.6	
$D_{K'}'$ (Hz)	0.73	0.05	
$d_{1'}'$ (Hz)	18	5	
$d_{2'}'$ (Hz)	-2	2	
κ'	-0.999		-0.999
$\Delta I'$ (amu \AA^2) ^d	-1.35	0.04	-3.76
assign	207		
rms (OMC)	5.3		

^a Numbers in parentheses represent estimates of the systematic uncertainties in the experiment. Band origin was not determined owing to the lack of a calibrated I_2 spectrum in this region. ^b Estimated errors from the diagonal elements of the correlation matrix. ^c Estimated by addition of a methyl group to the OT geometry obtained by Serrano-Andrés et al. (ref 16). ^d Neglecting distortion parameters.

This effect is so dramatic that the $K_a = 1$ and 2 subbands exhibit nearly identical shifts from the origin.

The most likely explanation of this effect is Coriolis coupling.¹⁹ The S_1 vibrational level reached in band NT-3, at $0_0^0 + 60.1\text{ cm}^{-1}$, is believed to be the analogue of the S_1 level in band OT-1 of octatetraene, a b_u bending mode. According to Petek et al.,⁷ it is nearly degenerate with the $3a_1$ methyl torsional level built upon the electronic origin of NT, at a (calculated) frequency of $0_0^0 + 63.2\text{ cm}^{-1}$. Therefore, it is reasonable to suppose that the two zero-order levels are coupled by a Coriolis interaction, leading to the observed perturbations in the spectrum, especially since these perturbations appear to be larger for odd K_a . (A first-order treatment of the Coriolis interaction in symmetric top molecules leads to terms in the rotational Hamiltonian that are linear in K_a .¹⁷) A more complete analysis of this behavior is in progress.

We turn next to the results for bands 2 and 4 of trans,trans-NT. These bands also are perturbed but for a different reason. The rotationally resolved spectrum of band NT-2, the blue member of the doublet located at $28\,954.1\text{ cm}^{-1}$, is shown in Figure 5. Our analysis of this spectrum reveals that each K_a

subband with $K_a \geq 1$ is split into two components, with the center of gravity of the two components shifting to the red with increasing $|K_a|$. Qualitatively similar behavior is exhibited by the K_a subbands in the rotationally resolved spectrum of the blue member of the doublet located at $29\,014.3\text{ cm}^{-1}$, band NT-4, as shown in Figure 6.

The origin of these perturbations is the torsion–rotation interaction.¹⁷ Recall that bands NT-2 and NT-4 have been assigned to transitions that connect the 1e methyl torsional component of the ZPL of the S_0 state with the corresponding components of two different vibrational levels of the S_1 state. As discussed in detail elsewhere,²⁰ the torsion–rotation interaction affects a and e torsional levels differently. The a torsional levels are affected only in second order, leading to modified values of their rotational constants, whereas the e torsional levels are affected both in first and in second order, leading to splittings that depend on K_a as well as modified rotational constants. The observation of such splittings in the high-resolution spectra of bands NT-2 and NT-4 thus confirms their assignment as 1e–1e bands.

We now use the observed splittings to obtain information about the barriers to internal rotation of the methyl group in the S_0 and S_1 states of *trans,trans*-NT. The effective Hamiltonian is

$$\hat{H} = \hat{H}_T + \hat{H}_R + \hat{H}_{TR} \quad (1)$$

where

$$\hat{H}_T = Fp^2 + V_3(1 - \cos 3\phi)/2 \quad (2)$$

$$\hat{H}_R = AP_a^2 + BP_b^2 + CP_c^2 \quad (3)$$

$$\hat{H}_{TR} = D_a P_a + D_b P_b \quad (4)$$

and the rest of the terms have their usual meaning.²⁰ We first fit the high-resolution spectra of bands NT-2 and NT-4 using eq 1 to model the rotational energy level patterns in the e torsional components of the connected vibrational levels of the two electronic states. This led to two sets of ground-state constants that were found to be identical within experimental error. Then we used the combination–difference method to extract more accurate values of the inertial parameters of the e subtorsional level of the ZPL of the S_1 state from the spectrum of band NT-2. A similar refinement of the fit of band NT-4 was not attempted owing to the presence of additional Coriolis perturbations in this spectrum.

Table 5 lists the values of the parameters that were derived using this procedure. Considering first the rotational constants of the a and e torsional components of the ZPL of the S_0 state, we see from a comparison of the values in Tables 3 and 5 that they are nearly the same within experimental error, showing that the second-order contribution of the torsion–rotation interaction is small in the ground state. Making the same comparison for the S_1 state (Tables 4 and 5), we see again that the C' rotational constants are the same but that the A' and B' rotational constants are significantly different, showing that the second-order contributions of the torsion–rotation interaction are large in this case, especially for motions about *a* and *b*. In this connection, it is interesting to note that the errors in the determinations of the *A* rotational constants of the e components of the ZPL's of the S_0 and S_1 states are very small, despite the near-symmetric-top nature of the spectra. This significant improvement in the accuracy of the experiment can be traced to a mixing of K_a , K_c states in the affected levels by the torsion–

TABLE 5: Inertial Parameters of *trans,trans*-Nonatetraene in the 1e Torsional Components of the Zero-Point Levels of Its Ground and First Excited Electronic States

	S_0 (“ 1^1A_g ”)		S_1 (“ 2^1A_g ”)	
	expt ^a	std error ^b	expt ^c	std error ^b
<i>A</i> (MHz)	16102	2.3	15419	2.5
<i>B</i> (MHz)	390.23(0.1)	0.02	383.85(0.1)	0.03
<i>C</i> (MHz)	382.07(0.1)	0.02	375.70(0.1)	0.03
D_x (MHz)			200.3	0.05
D_z (MHz)	0.19	0.62	15428.5	0.2
D_z^3 (MHz)			−99.42	0.06
κ	−0.999		−0.999	
ΔI (amu \AA^2) ^d	−3.56	0.08	−4.2	0.4

^a Results from a fit of 423 combination–differences that appear in the rotationally resolved spectra of the two blue components of the doublets that appear in the 0_0^0 and $0_0^0 + 60.1\text{ cm}^{-1}$ bands, located at $28\,954.1$ and $29\,014.3\text{ cm}^{-1}$, respectively, using the torsion–rotation Hamiltonian (eq 1). Numbers in parentheses represent estimates of the systematic uncertainties in the experiment. Band origin was not determined owing to the lack of a calibrated I_2 spectrum in this region.

^b Estimated errors from the diagonal elements of the correlation matrix.

^c Results from a fit of 159 assigned transitions in the spectrum of band NT-2, the blue component of the doublet of the 0_0^0 band, located at $28\,954.1\text{ cm}^{-1}$. The ground-state parameters were fixed to the values shown in this table. The standard deviation of this fit is 7.03 MHz.

^d Neglecting internal rotation parameters.

rotation interaction.²⁰ These perturbations cause a splitting of the nearly degenerate rotational levels differing only in K_c , which are exactly degenerate in the symmetric top limit. Increases in these splittings relative to the resolution of the experiment provide increased accuracies of the determinations of the *A* constants of the affected vibrational levels.

Considering next the first-order torsion–rotation constants in Table 5, we find $D_x'' = 0$ and $D_z'' = 0.19\text{ MHz}$ for the e component of the S_0 state and $D_x' = 200$ and $D_z' = 15\,430\text{ MHz}$ for the e component of the S_1 state. The first-order term D_z' is very large, as large as the A' rotational constant itself, requiring the inclusion in eq 4 of a third-order correction term (which is neglected in the subsequent analysis). These data show that there is a large decrease in the methyl internal rotation barrier in the S_1 state. Combining the data in the usual way²⁰ and using as well the observed tunneling splittings in the low-resolution spectrum,⁷ we find $V_3(S_0) \geq 900\text{ cm}^{-1}$, and $V_3(S_1) = 42.8$ and $V_6(S_1) = -29.4\text{ cm}^{-1}$. (The V_6 term was added to eq 2 to improve the fit.) These values are in good agreement with those determined by Petek et al.⁷ Thus, the observed tunneling splittings are almost entirely attributable to a low torsional barrier in the S_1 state.

Finally, we turn to DT. Figure 7 shows the high-resolution spectra of two members (DT-1 and DT-2) of the triplet observed in the DT $S_1 \leftarrow S_0$ spectrum located at $29\,014.0$ and $29\,017.1\text{ cm}^{-1}$. (DT-3 was not recorded owing to its low intensity.) Given the results for OT and NT, it is reasonable to expect (as did Petek et al.^{6,7}) that bands DT-1, 2, and 3 are the tunneling “triplet” of the vibronic origin of DT, 50.9 cm^{-1} above the true origin of the $S_1 \leftarrow S_0$ transition. Examination of Figure 7 shows that these two observed bands conform qualitatively to this expectation. Both are a-type bands. Band DT-1 appears to be a $0a_1 \leftarrow 0a_1$ transition, unperturbed by torsion–rotation coupling, and band DT-2 appears to be a significantly perturbed $1g \leftarrow 1g$ transition. Apparently, the species responsible for these bands is *trans,trans*-DT. Unfortunately, both bands are too weak to permit detailed analysis at this time. This is probably a result of several factors. Addition of the second methyl group has restored the center of inversion that makes the $S_1 \leftarrow S_0$ transition forbidden in the C_{2h} point group. In addition, its intensity is

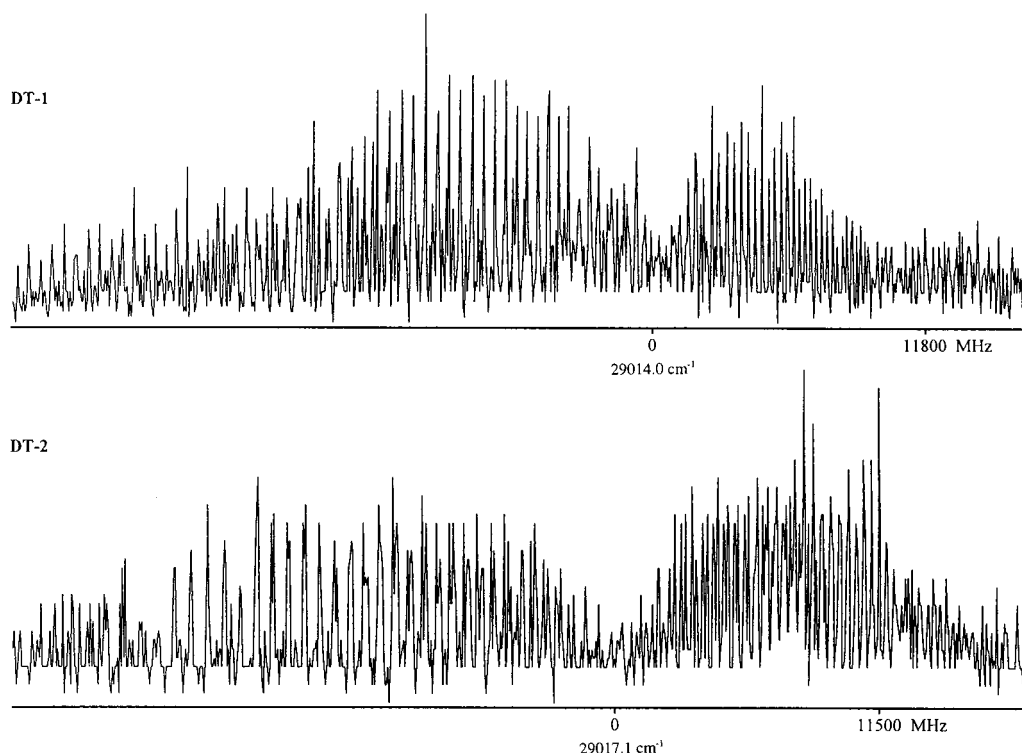


Figure 7. High-resolution one-photon fluorescence excitation spectra of bands DT-1 and DT-2 in the $S_1 \leftarrow S_0$ transition of decatetraene in a molecular beam. The two bands are centered at 29 014.0 and 29 017.1 cm^{-1} , respectively.

now spread over three torsional levels having different nuclear spin symmetries. And perhaps most importantly, the vapor pressure decreases as one goes from OT to DT, resulting in progressively lower concentrations in the molecular beam. Owing to the instability of these compounds, this cannot be compensated for by heating.

The inability to observe the blue member of the triplet, DT-3, may indicate the existence of a coupling between the two methyl rotors, despite their large separation. In the absence of such coupling, consideration of nuclear spin statistics suggests that the relative intensities of bands DT-1 and DT-3 should be the same. However, in the presence of such coupling, the normally degenerate members of an e torsional level, associated with clockwise and counterclockwise rotations of the first methyl group, would have different energies, depending on the sense of rotation of the second methyl group. A splitting would result, leading to a further diminution of the intensities of the affected band, DT-3 in this case. As shown elsewhere,²¹ the bands of two coupled rotors also would be expected to exhibit significant torsion-rotation interactions, especially for rotors that are hindered by only small barriers.

Discussion

Eight vibronic bands in the $2^1A_g - 1^1A_g$ electronic transitions of OT, NT, and DT have been recorded at high resolution. Given the thermal instability of the compounds, their near-symmetric-top nature, and the existence of several perturbations, the analyses of these spectra posed significant challenges. Nevertheless, five of the bands have been fully assigned and three have been partially analyzed, providing valuable new information about these polyenes in their ground and first electronically excited states.

Paramount among our findings are the rotational constants of OT and NT in their ground electronic (1^1A_g) states (Tables 1, 3, and 5). Alone among all known spectroscopic parameters of an isolated molecule in the gas phase, its rotational constants

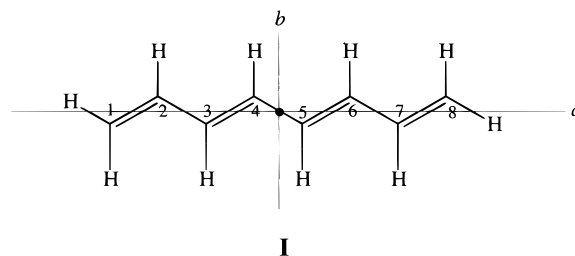
are the most sensitive to its three-dimensional structure. This information is contained in its principal moments of inertia I_a , I_b , and I_c , which are related to its rotational constants A , B , and C by

$$I_a = \frac{h}{8\pi^2 A}, \text{ etc.} \quad (5)$$

and to the displacements of each of its component atomic masses from the relevant axes by

$$I_a = \sum_i m_i (b_i^2 + c_i^2), \text{ etc.} \quad (6)$$

Thus, the fact that OT has a large A constant is a consequence of its small moment of inertia I_a ; the displacements of each of the C and H atoms from the a axis (b_i and c_i) are all relatively small (\AA). In contrast, OT has relatively small B and C constants



because the displacements of many of the atoms from the b and c axes are relatively large.

Three rotational constants are clearly insufficient to determine the complete structure of OT and its derivatives, making necessary a comparison with theory in order to establish the identity of the species responsible for the spectra. Fortunately, this comparison leads to an unambiguous result. OT has 20 distinguishable isomers, 15 including *cis*³ configurations.²

TABLE 6: Modeling the Geometry of *trans,trans*-Octatetraene in Its Ground (1^1A_g) and Electronically Excited (2^1A_g) States

parameter ^a	S_0 (1^1A_g)		S_1 (2^1A_g)		
	model 1	CASSCF ^b	model 2	model 3	CASSCF ^b
$r_1(C_1-C_2)$	1.340	1.343	1.460	1.460	1.438
$r_2(C_2-C_3)$	1.460	1.456	1.340	1.340	1.376
$r_3(C_3-C_4)$	1.340	1.349	1.460	1.460	1.437
$r_4(C_4-C_5)$	1.460	1.452	1.340	1.340	1.392
$\angle_1(C_1-C_2-C_3)$	124.0	124.3	124.0	125.2	124.5
$\angle_2(C_2-C_3-C_4)$	124.0	124.0	124.0	125.2	124.3
$\angle_3(C_3-C_4-C_5)$	124.0	124.1	124.0	125.2	124.1
A (MHz)	19,574	19,738	19,711	20,146	19,649
B (MHz)	570.5	568.0	562.6	555.9	555.8
C (MHz)	554.4	552.2	547.0	540.9	540.5

^a Bond lengths in angstroms and bond angles in degrees. A C-H bond length of 1.078 Å and H-C-C angles of $1/2(360 - \angle C-C-C)^\circ$ were used in all calculations. ^b CASSCF/ANO results (ref 16).

However, only the *trans,trans* form (**I**) has calculated B'' and C'' rotational constants that agree with those measured in this work. For NT, the best agreement between experiment and theory also is obtained for the *trans,trans* isomer. Here, we find from our fit of band NT-2 the values $A'' = 16\,102 \pm 2.3$, $B'' = 390.2 \pm 0.1$, and $C'' = 382.1 \pm 0.1$ MHz, whereas theory (CASSCF)¹⁶ gives the values $A'' = 16\,090$, $B'' = 390.0$, and $C'' = 381.9$ MHz. Thus, we confirm the conclusions of Petek et al.⁵⁻⁷ The carriers observed in their spectra of OT, NT, and DT are primarily the *trans,trans* forms. These data also show that modern ab initio theory gives an accurate description of the structures of the isolated molecules in their ground electronic states.

Now, the patterns of energy levels observed in the high-resolution spectra also are sensitive to the size and shape of the molecules in their electronically excited states and therefore to the *changes* in structure that occur when the photon is absorbed. We find (Tables 2, 4, and 5) that excitation of all three molecules to their S_1 (2^1A_g) states results in large increases in A and small decreases in B and C . This shows that the molecular dimensions perpendicular to a decrease significantly while those perpendicular to b and c increase slightly, compared to the ground state. Despite uncertainties in the A' constants themselves, the *changes* in the rotational constants, $\Delta A (= A' - A'')$, ΔB , and ΔC , are all known to high precision (± 0.1 MHz). These are 2532, -11.7 , and -11.0 MHz for the $0_0^0 + 76.2$ cm^{-1} band of OT; 2243, -11.7 , and -11.1 MHz for the $0_0^0 + 411.9$ cm^{-1} band of OT; and 457, -6.3 , and -6.5 MHz for the 0_0^0 band of NT, respectively. The magnitudes of the changes are smaller in NT. Ab initio theory¹⁶ predicts the values $\Delta A = -88.8$, $\Delta B = -12.3$, and $\Delta C = -11.7$ MHz for *trans,trans*-OT. The agreement between the observed and calculated values of ΔB and ΔC is very good. However, the difference between the observed and calculated ΔA values is very large, much too large to be attributed to the vibrational contributions of an in-plane bending motion²² and/or possible inadequacies of the distortable rotor Hamiltonian. In all cases, we find $\Delta A > 0$, whereas theory predicts $\Delta A < 0$.²³ This shows that modern ab initio descriptions of the structures of the excited electronic states of isolated polyenes are still inadequate.

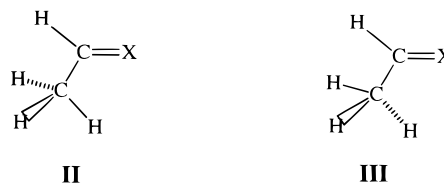
Intrigued by this result, we have performed some simple calculations to explore the connections between different model OT geometries and their rotational constants. The properties of the model structures are listed in Table 6. For the ground state (model 1), we chose $r_1(C_1-C_2) = r_3 = 1.340$ Å, $r_2 = r_4 = 1.460$ Å, and $\angle_1 = \angle_2 = \angle_3$ (C-C-C) = 124.0° , thereby capturing the essence of its structure, alternating C-C bond

lengths and C-C-C angles close to 120° . The specific values of these parameters were chosen to most closely match those of the CASSCF geometry of the ground state,¹⁶ also listed in Table 6. We ignore the small calculated decrease in the difference between "single" and "double" bond lengths as one moves toward the center of the structure, and the small differences in the bond angles. Despite these facts, model 1 has the rotational constants $A'' = 19\,574$, $B'' = 571$, and $C'' = 554$ MHz, in reasonable agreement with the experimental results.

Next, we distorted the molecule along one or more of the chosen coordinates to model its possible behavior on excitation to the S_1 state. According to theory,^{16,24,25} the primary characteristic of the $S_1 \leftarrow S_0$ transition in the polyenes is bond-order "reversal". Thus, as shown in Table 6, the CASSCF calculation¹⁶ predicts that single bonds shorten and double bonds lengthen on S_1 excitation, whereas the C-C-C angles remain essentially unchanged. Model 2 was chosen to mimic this behavior. Here, we find that decreasing r_2 and r_4 from 1.460 to 1.340 Å increases A , B , and C , owing to decreases in the displacements of all atoms from all three inertial axes. Increasing r_1 and r_3 from 1.340 to 1.460 Å has the opposite effect. But the magnitudes of the observed changes in $A-C$ are different in the two cases, since OT (in its ground state) has fewer C-C single bonds than double ones. Thus, when we simultaneously increased r_1 and r_3 while decreasing r_2 and r_4 , we found that A increases while B and C decrease. The primary reason for the increase in A is that a decrease in r_4 moves *all* atoms closer to the a axis.

The model 2 structure, with $r_1 = r_3 = 1.460$ Å, $r_2 = r_4 = 1.340$ Å, and $\theta = 124^\circ$, has $\Delta A = 137$, $\Delta B = -7.9$, and $\Delta C = -7.4$ MHz. To improve the agreement with experiment, we also explored the effect of changes in the C-C-C bond angles. Increasing these angles increases A , since the displacements of the atoms with respect to a decrease, and decreases B and C , since the displacements with respect to b and c increase. Our model 3 structure, which has all C-C-C angles set to 125.2° , has $\Delta A = 572$, $\Delta B = -14.6$, and $\Delta C = -13.5$ MHz. The calculated ΔA value is still in rather poor agreement with the observed one. Nonetheless, it is large and positive, as observed. Thus, it appears that S_1 excitation of the typical polyene results in significant changes in the bond angles as well as the bond lengths. Studies of isotopically labeled species and/or further refinements of theory will be necessary to confirm this finding.

Another dramatic consequence of the change in electronic structure on $S_1 \leftarrow S_0$ excitation is the large decrease in the methyl group internal rotation barriers in NT and DT. We find $V_3(S_0) \geq 900$ cm^{-1} ; $V_3(S_1) = 42.8$ and $V_6(S_1) = -29.4$ cm^{-1} in NT. Petek et al.⁷ find comparable values for NT and DT from their analyses of the low-resolution spectra. Now it is known that the ground states of propene and other molecules having $\text{CH}_3\text{-CH}=\text{X}$ functionalities prefer methyl group conformations that have a C-H bond *syn* or eclipsed with the double bond, as shown below (**II**). The barrier to rotation is on



the order of 700 cm^{-1} . The origin of this barrier can be traced to repulsive interactions between the occupied methyl group orbitals of π symmetry and the π orbitals of $\text{C}=\text{X}$.²⁶ However, the situation is different in $\pi\pi^*$ excited states. Here, the staggered conformation (**III**) is preferred because the dominant interaction is an attractive one, owing to overlap of the singly

occupied $\pi^*_{\text{C}=\text{C}}$ orbital and the vacant $\pi^*_{\text{CH}_3}$ orbital.²⁶ Thus, the magnitude (and sign) of the methyl group internal rotation barrier is a sensitive probe of the π -orbital bond order in the adjacent C=C bond(s).^{20,27}

Theory (HF/6-31G*)¹⁸ predicts that the stable conformation of NT in its ground electronic state is the eclipsed form **II**, consistent with the existence of a double bond between C₇ and C₈ and with its measured torsional barrier in the S₀ state. However, this barrier drops precipitously on excitation to the S₁ state. This shows that there is a large decrease in the π bond order in the adjacent C=C bond in the S₁ state. Thus, the small torsional barrier in the S₁ state of NT also provides compelling evidence for bond order reversal in the S₁ ← S₀ transitions of these linear polyenes. The C₇=C₈ bond in trans,trans-NT must be nearly a single bond in the S₁ state.

It is interesting to note that the methyl group internal rotation barrier in the S₁ state of trans,trans-NT ($V_3 = 42.8$, $V_6 = -29.4$ cm⁻¹) is comparable to that of the ethyl radical, in its ground state ($V_3 \leq 50$ cm⁻¹).²⁸ As is well-known, Hudson and Kohler²⁹ were the first to show that the S₁ state of most linear polyenes is a mixture of singly and doubly excited A_g configurations rather than the singly excited B_u (HOMO–LUMO) configuration predicted by simple MO theory. Theoretical calculations by Schulten et al.²⁴ confirmed this conclusion. One chemical consequence of this finding is bond-order reversal. A second consequence is two “separated but paired” electrons, mostly localized on the terminal carbon atoms in the S₁ state. The ethyl radical also has a largely localized (unpaired) electron, in a π -type orbital adjacent to the CH₃ group. Thus, the fact that the internal rotation barriers in these two species are similar suggests that, in accord with theory, the S₁ state of trans,trans-NT also has “single” π electrons localized on C₁ and C₈. The measured barrier is a very sensitive probe of the interaction of these electrons with attached methyl groups.

The rotationally resolved spectra presented in this work also provide compelling evidence for the model proposed by Petek et al.^{5–7} to explain the source of S₁ ← S₀ oscillator strength in trans,trans-OT, NT, and DT. This information comes from our analysis of the two bands of OT, in which it was found that the two excited-state vibrational levels have unusually large values of the centrifugal distortion term D_K' (10.4 MHz in band OT-1 and 13.7 MHz in band OT-2; Table 2). Both levels exhibit small, positive inertial defects (1.08 and 0.80 amu Å², respectively), whereas the ZPL of the S₀ state exhibits a small, negative ΔI value (−2.14 amu Å²). Both in-plane and out-of-plane vibrations contribute to the inertial defects of planar molecules.¹⁷ Usually, in-plane vibrations make a positive contribution and out-of-plane vibrations make a negative contribution. We believe, therefore, that out-of-plane vibrations dominate in the ZPL of the S₀ state, given its observed negative inertial defect. Further, since the sign of ΔI changes on excitation of trans,trans-OT to both of the two examined S₁ vibrational levels, we also believe that these two levels involve significant in-plane motions.

C₈H₁₀ has 48 (nondegenerate) vibrational modes, 33 in-plane (a_g and b_u) and 15 out-of-plane (a_u and b_g).⁹ Six in-plane modes have frequencies less than 600 cm⁻¹ in the ground state. These are all C–C–C bending modes: ν_{15} (a_g) at 543, ν_{16} (a_g) at 332, ν_{17} (a_g) at 222, ν_{46} (b_u) at 566, ν_{47} (b_u) at 390, and ν_{48} (b_u) at 86 cm⁻¹. (The quoted frequencies are scaled MP2/6-31G* values.³⁰) Given the frequency displacements in the spectra (76 and 412 cm⁻¹), the observed levels are likely the excited-state analogues of two of these modes or linear combinations of them (owing to possible Duschinsky rotations). Petek et al.⁵ have assigned them as ν_{48} and $\nu_{48} + \nu_{16}$, placing ν_{48} at 76.2 and ν_{16}

at 335.7 cm⁻¹ in the S₁ state, close to the ground-state values. However, significant changes in both the nature and the frequencies of these modes could occur on S₁ excitation.

The values of the quartic distortion terms derived from the fits of bands OT-1 and OT-2 provide new information about the identity of these modes. The largest distortion term by far is $D_{K'}$, which is at least 3 orders of magnitude larger than D_J' and $D_{JK'}$, and much larger than in other “typical” large molecules. Thus, if the source of this nonrigid behavior were a genuine centrifugal effect, we would conclude that the largest force produced by rotation is for rotation about the *a* axis, when K_a is large. That rotation of OT about its (near) symmetric top axis could lead to distortions of the molecule in directions perpendicular to the axis of rotation is reasonable. But the $D_{K'}$ value of NT in the ZPL of its S₁ state, where similar effects might be expected, is relatively small, $D_{K'} = 0.73$ MHz (Table 4). Further, only g vibrational modes can be involved in centrifugal distortion.³¹ Therefore, it is likely that the large $D_{K'}$ values for bands OT-1 and OT-2 of octatetraene are not truly centrifugal in origin but instead are due to Coriolis coupling involving ν_{48} and an out-of-plane vibration. This vibration must be of a_u symmetry to couple about the *a* axis. As suggested by Watson,³¹ this mechanism also would explain why ΔA for OT is unexpectedly large.

The approximate Hamiltonian for the *K* rotational energies is³¹

$$E(K) = \begin{bmatrix} \nu_{48} + AK^2 & 2iA\zeta K \\ -2iA\zeta K & \nu_{25} + AK^2 \end{bmatrix} \quad (7)$$

Expanding yields

$$E(K) = \nu_{48} + AK^2 + \frac{4A^2\zeta^2 K^2}{\nu_{48} - \nu_{25}} - \frac{16A^4\zeta^4 K^4}{(\nu_{48} - \nu_{25})^3} + \dots \quad (8)$$

Here, ν_{25} is the frequency of an a_u out-of-plane bending mode, calculated to be 60 cm⁻¹.³⁰ If we take $\Delta A = 2$ GHz, $A = 20$ GHz, and $\nu_{48} - \nu_{25} = 16$ cm⁻¹, we find from eq 8 the Coriolis parameter $\zeta = 0.77$, a not unreasonable result. Therefore, we conclude that the large value of $D_{K'}$ in band OT-1 is most likely a consequence of Coriolis effects involving ν_{48} and ν_{25} . A similar explanation would account for the large $D_{K'}$ value in band OT-2, in which $\nu_{48} + \nu_{16}$ interact with $\nu_{25} + \nu_{16}$. We further conclude that such couplings also could account for the large ΔA values of these two bands. And finally, we confirm the suggestion of Petek et al.,⁵ band OT-1 terminates in the analogue of the “overall” b_u in-plane bending mode (ν_{48}) in the S₁ state.

This spectroscopic finding has significant implications for the properties of the isolated molecule. As shown by Petek et al.,⁵ the origin in the two-photon excitation spectrum of octatetraene is ~ 76 cm⁻¹ lower in energy than the origin of the one-photon spectrum. We have shown that the latter band originates in the ZPL of the S₀ state of the trans,trans form, is an *a*-type spectrum,^{32,33} and terminates in a vibronic level of the S₁ state that has b_u symmetry, lying ~ 76 cm⁻¹ above the ZPL. Thus, this band (OT-1 at 0₀⁰ + 76.2 cm⁻¹) is the “false” origin of the S₁ ← S₀ transition of trans,trans-OT. It gains its intensity via Herzberg–Teller coupling with the S₂ (1¹B_u) state, via the b_u promoting mode, which is the origin of most of the remaining vibrational activity in the spectrum.⁵ As also shown by Petek et al.,⁵ the complete lack of overlap between vibronic bands in the one- and two-photon spectra proves that the one-photon (g → u) and two-photon (g → g) selection rules are strictly obeyed, thus excluding a *cis* form of OT as the carrier of the spectrum.

It is interesting to note that the CASSCF geometry of the 1^1B_u state of *trans,trans*-OT has rotational constants of $A = 20\,148$, $B = 559$, and $C = 544$ MHz.^{16,18} The calculated values of B and C for the 1^1B_u state are nearly the same as those for the 2^1A_g state. However, the calculated value of A for the 1^1B_u state is significantly larger than the corresponding value for the 2^1A_g state. Thus, if the degree of mixing of the two states via the b_u promoting mode is large, this may account for at least some of the discrepancy between the observed and calculated values of ΔA for the 2^1A_g state.

Making such arguments quantitative is a challenging task.³⁴ In early work, Kohler and co-workers^{35–37} invoked vibronic coupling between the ground 1^1A_g and excited 2^1A_g states to explain the increase in frequency of the Franck–Condon active, totally symmetric C=C stretch that was observed on excitation of 2,10-dimethylundecapentaene and 2,12-dimethyltridecahexaene. Later, Orlandi and Zerbetto³⁸ showed that, whereas vibronic couplings between states of the same parity are strong and are caused predominantly by C–C stretching modes, the couplings between states of opposite parity are comparatively weak and involve mainly C–C–C bending modes. More recently, Buma and Zerbetto³⁹ used CI methods to investigate vibronic intensity patterns in the spectrum of *trans,trans*-OT. They found that the low-frequency b_u mode (ν_{48}) is most active in coupling the two 1^1A_g and 1^1B_u states. They also confirmed that the intensity of the false origin in the one-photon excitation spectrum of *trans,trans*-OT is comparable to that of the true origin in an OT containing a *cis* linkage, as previously discussed by Petek et al.⁵ Future modeling of this effect should focus on *trans,trans*-NT, in which both the true and false origins are observed (cf., Figure 1). Quantitative estimates of the vibronic coupling matrix elements are needed to account for the large variations in time scales that have been observed in the excited-state relaxation behavior of several polyenes.⁴⁰

Conclusions

Rotationally resolved electronic spectra of several vibronic bands in the $S_1 \leftarrow S_0$ transitions of octatetraene (OT), nonatetraene (NT), and decatetraene (DT) in the gas phase have been observed and analyzed. These analyses show that (1) the first strong band in the one-photon spectrum of OT originates in the zero-point vibrational level (ZPL) of the ground (1^1A_g) state of the *trans,trans* isomer and terminates in the ν_{48} vibrational level of the excited (2^1A_g) state, which lies ~ 76 cm^{-1} above its ZPL, (2) the one-photon spectrum, strictly forbidden by parity selection rules, gains its intensity via Herzberg–Teller coupling with the S_2 (1^1B_u) state, via the ν_{48} (b_u) promoting mode, (3) the S_1 state of *trans,trans*-OT has a different equilibrium geometry from that of the S_0 state, exhibiting significant changes in the C–C–C bond angles as well as the C–C bond lengths, as required by bond-order reversal models of the S_1 state, (4) the first two strong bands in the one-photon spectrum of NT originate in the ZPL of the ground (1^1A_g) state of the *trans,trans* isomer and terminate in the ZPL and ν_{48} vibrational levels of the excited (2^1A_g) state, which lies ~ 60 cm^{-1} above its ZPL (the two bands are, respectively, the true and false origins of the $S_1 \leftarrow S_0$ transition, the former being no longer strictly forbidden), and (5) the methyl group internal rotation barrier in *trans,trans*-NT, large in the S_0 state, decreases significantly on excitation to the S_1 state, further validating the bond reversal model. The observed spectra of DT are consistent with its assignment to the *trans,trans* structure. All of these conclusions agree with the earlier assignments and interpretations of Petek et al.^{5–7} The excited-state rotational constants

and other experimental parameters derived in this work will serve as benchmarks for future theoretical studies of the structural and dynamical properties of linear polyenes.

Acknowledgment. The entire scientific community was saddened by the loss of Bryan Kohler. He was a good friend. Additionally, he inspired all of us with his infectious enthusiasm for science and the challenges it presents. One of those challenges was posed by the results described herein; while they disagreed with his own work, no one was more interested in discussing them. Therefore, we are most pleased to dedicate this work to his memory, acknowledging in this small way Bryan's immense contributions to science and to the lives of those fortunate enough to work with him. We are grateful to Bryan and to B. Champagne, H. Petek, A. Stolow, X.-Q. Tan, and J. Watson for many helpful conversations about this work. T. Korter assisted with some of the calculations. J. Watson provided the model described in eqs 7 and 8. This research has been supported by NSF (CHE-9224398, CHE-9617208) and by a grant from the Pittsburgh Supercomputing Center. Acknowledgment is also made to the donors of the Petroleum Research Fund, administered by the ACS, for partial support of this research.

References and Notes

- (1) For reviews, see the following. Hudson, B. S.; Kohler, B. E.; Schulten, K. *Excited States*; Lim, E. C., Ed.; Academic Press: New York, 1982; Vol. 6, p 1. Kohler, B. E. *Chem. Rev.* **1993**, *93*, 41.
- (2) Yeh, C.-Y. *J. Chem. Phys.* **1996**, *105*, 9706.
- (3) Heimbrook, L. A.; Kohler, B. E.; Levy, I. J. *J. Chem. Phys.* **1984**, *81*, 1592.
- (4) Buma, W. J.; Kohler, B. E.; Shaler, T. A. *J. Chem. Phys.* **1992**, *96*, 399.
- (5) Petek, H.; Bell, A. J.; Choi, Y. S.; Yoshihara, K.; Tounge, B. A.; Christensen, R. L. *J. Chem. Phys.* **1993**, *98*, 3777.
- (6) Petek, H.; Bell, A. J.; Yoshihara, K.; Christensen, R. L. *J. Chem. Phys.* **1991**, *95*, 4739.
- (7) Petek, H.; Bell, A. J.; Choi, Y. S.; Yoshihara, K.; Tounge, B. A.; Christensen, R. L. *J. Chem. Phys.* **1995**, *102*, 4726. Slightly different values of the tunneling splittings of nonatetraene were determined from analysis of the high-resolution spectra. See Figures 4–6.
- (8) Pratt, D. W. *Annu. Rev. Phys. Chem.* **1998**, *49*, 481.
- (9) Yoshida, H.; Tasumi, M. *J. Chem. Phys.* **1988**, *89*, 2803.
- (10) Majewski, W. A.; Pfanstiel, J. F.; Plusquellic, D. F.; Pratt, D. W. *Laser Techniques in Chemistry*; Rizzo, T. R., Myers, A. B., Ed.; J. Wiley & Sons: New York, 1995; p 101.
- (11) Previously published, without analysis. Mukamel, S. *Principles of Nonlinear Optical Spectroscopy*; Oxford, U.K., 1995.
- (12) Pfanstiel, J. F.; Champagne, B. B.; Majewski, W. A.; Plusquellic, D. F.; Pratt, D. W. *Science* **1989**, *245*, 736.
- (13) Champagne, B. B.; Pfanstiel, J. F.; Plusquellic, D. F.; Pratt, D. W.; van Herpen, W. M.; Meerts, W. L. *J. Phys. Chem.* **1990**, *94*, 6.
- (14) Watson, J. K. G. *J. Chem. Phys.* **1967**, *46*, 1935. Watson, J. K. G. *Vibrational Spectra and Structure*; Durig, J. R., Ed; Elsevier: Amsterdam, 1977; Vol. 6, p 1.
- (15) Frisch, M. J.; Trucks, G. W.; Head-Gordon, M.; Gill, P. M. W.; Wong, M. W.; Foresman, J. B.; Johnson, B. G.; Schlegel, H. B.; Robb, M. A.; Replogle, E. S.; Gomperts, R.; Andres, J. L.; Raghavachari, K.; Binkley, J. S.; Gonzalez, C.; Martin, R. L.; Fox, D. J.; Defrees, D. J.; Baker, J.; Stewart, J. J. P.; Pople, J. A. *Gaussian 92*, revision E.1; Gaussian, Inc.: Pittsburgh, PA, 1992.
- (16) Serrano-Andrés, L.; Lindh, R.; Roos, B. O.; Merchán, M. *J. Phys. Chem.* **1993**, *97*, 9360.
- (17) Gordy, W.; Cook, R. L. *Microwave Molecular Spectra*, 3rd ed.; Wiley-Interscience: New York, 1984.
- (18) Pfanstiel, J. F. Ph.D. Thesis, University of Pittsburgh, 1994.
- (19) Herzberg, G. *Infrared and Raman Spectra*; D. van Nostrand Co., Inc.: Princeton, NJ, 1945.
- (20) Tan, X.-Q.; Majewski, W. A.; Plusquellic, D. F.; Pratt, D. W. *J. Chem. Phys.* **1991**, *94*, 7721.
- (21) Tan, X.-Q.; Clouthier, D. J.; Judge, R. H.; Plusquellic, D. F.; Tomer, J. L.; Pratt, D. W. *J. Chem. Phys.* **1991**, *95*, 7862.
- (22) The vibrational contributions of ν_{48} to the rotational constants of the ground state are estimated to be $\Delta A = -1402$, $\Delta B = +3$, and $\Delta C =$

+3 MHz from the HF/6-31G* calculations (ref 18). Thus, ΔA , although having the right order of magnitude, has the wrong sign to explain this discrepancy.

(23) Negative ΔA values have been found in DPB (ref 12) and *tS* (ref 13), but in these cases the observed changes appear to be associated primarily with increases in the lengths of the C—C bonds in the phenyl rings that are most perpendicular to *a*.

(24) Schulten, K.; Ohmine, I.; Karplus, M. *J. Chem. Phys.* **1976**, *64*, 4422. See also the following. Schulten, K.; Karplus, M. *Chem. Phys. Lett.* **1972**, *14*, 305.

(25) Aoyagi, M.; Ohmine, I.; Kohler, B. E. *J. Phys. Chem.* **1990**, *94*, 3922.

(26) Dorigo, A. E.; Pratt, D. W.; Houk, K. N. *J. Am. Chem. Soc.* **1987**, *109*, 6591.

(27) For a review, see the following. Spangler, L. H.; Pratt, D. W. *Jet Spectroscopy and Molecular Dynamics*; Hollas, J. M., Phillips, D., Ed.; Chapman & Hall: London, 1995; p 366.

(28) Chipman, D. M. *J. Chem. Phys.* **1991**, *94*, 6632. Nesbitt, D. J. Unpublished results. Sears, T. J. Unpublished results.

(29) Hudson, B. S.; Kohler, B. E. *Chem. Phys. Lett.* **1972**, *14*, 299.

(30) Hirata, S.; Yoshida, H.; Torii, H.; Tasumi, M. *J. Chem. Phys.* **1995**, *103*, 8955.

(31) Watson, J. K. G. Private communication.

(32) In this connection, it is interesting to note that we find no evidence for an "off-axis" orientation of the $S_1 \leftarrow S_0$ transition moment in any of our spectra, such as has been observed for some linear conjugated polyenes as guests in the channels of urea crystals by Hudson and co-workers (ref 33). However, we cannot rule out the possible existence of such a tilt; it could be as large as 15°.

(33) Shang, Q. Y.; Dou, X.; Hudson, B. S. *Nature (London)* **1991**, 352, 703. Dou, X.; Shang, Q. Y.; Hudson, B. S. *Chem. Phys. Lett.* **1992**, 189, 48. Lee, S. K.; Shang, Q. Y.; Hudson, B. S. *Mol. Cryst. Liq. Cryst.* **1992**, *211*, 147.

(34) See the following for an early review. Orlandi, G.; Zerbetto, F.; Zgierski, M. Z. *Chem. Rev.* **1991**, *91*, 867.

(35) Christensen, R. L.; Kohler, B. E. *J. Chem. Phys.* **1975**, *63*, 1837.

(36) Christensen, R. L.; Kohler, B. E. *J. Phys. Chem.* **1976**, *80*, 2197.

(37) Auerbach, R. A.; Christensen, R. L.; Granville, M. F.; Kohler, B. E. *J. Chem. Phys.* **1981**, *74*, 4.

(38) Orlandi, G.; Zerbetto, F. *Chem. Phys. Lett.* **1986**, *131*, 409.

(39) Buma, W. J.; Zerbetto, F. *J. Chem. Phys.* **1995**, *103*, 10492.

(40) Cyr, D. R.; Hayden, C. C. *J. Chem. Phys.* **1996**, *104*, 771. Blanchet, V.; Stolow, A. Submitted for publication.